Journal of
Composites Science

Article

Investigation of Solar Air Collectors with Carbon-Nanotube-Based Turbulators and Pin Fin Arrangements

M. Appadurai [1], E. Fantin Irudaya Raj [2], Vishal Ram [3], Augustine Mathu Gnaniah [3], Surender Reddy Salkuti [4,*] and Seong-Cheol Kim [4]

1 Department of Mechanical Engineering, Nehru College of Engineering & Research Centre, Thrissur 680588, India; appadurai4050.me@ncerc.ac.in
2 Department of Electrical and Electronics Engineering, Dr. Sivanthi Aditanar College of Engineering, Tiruchendur 628215, India; fantinirudhayaraj@drsacoe.com
3 Department of Electrical Engineering, Loyola-ICAM College of Engineering and Technology, Chennai 600034, India; vishalram.22ee@licet.ac.in (V.R.); augustine.m@licet.ac.in (A.M.G.)
4 Department of Railroad and Electrical Engineering, Woosong University, Jayang Dong, Dong-Gu, Daejeon 34606, Republic of Korea; kmin@wsu.ac.kr
* Correspondence: surender@wsu.ac.kr

Abstract: This research attempts to investigate the thermal performance of solar air collectors with pin fins and turbulators. Incorporating carbon-nanotube-based fins and turbulators in solar collectors can enhance their performance due to their high thermal conductivity, low weight, and high aspect ratio. In the present study, numerical analyses of a solar collector with pin fins and turbulators are carried out to investigate its effect on the Nusselt number. The paper begins with the numerical analysis of conventional air collectors and compares them with theoretical results. This is followed by numerical analyses, which are carried out to examine different configurations of the absorber plate with pin fins of varying diameters (10 mm, 20 mm, and 30 mm) and turbulators of varying heights (20 mm, 40 mm, and 60 mm) in the base plate. The analyses include variations in the Reynolds number ranging from 3000 to 15,000. Subsequently, after the performance of the solar collector with pin fins is evaluated, the effect of turbulators of varying heights on the Nusselt number is analyzed, followed by the analysis of the combined effect of pin fins and turbulators. The results are compared with traditional solar collectors and show that the combined effect of pin fins and turbulators can significantly improve the thermal performance of solar air collectors. The findings of this study can contribute to the development of renewable energy-based air conditioning, ventilation, and heating systems.

Keywords: solar air collectors; carbon nanotube (CNT); turbulators; pin fins; computational fluid dynamic (CFD) study; numerical analysis

Citation: Appadurai, M.; Raj, E.F.I.; Ram, V.; Gnaniah, A.M.; Salkuti, S.R.; Kim, S.-C. Investigation of Solar Air Collectors with Carbon-Nanotube-Based Turbulators and Pin Fin Arrangements. *J. Compos. Sci.* **2023**, *7*, 322. https://doi.org/10.3390/jcs7080322

Academic Editor: Francesco Tornabene

Received: 22 June 2023
Revised: 29 July 2023
Accepted: 2 August 2023
Published: 5 August 2023

1. Introduction

Solar energy is currently the second largest by cumulative power capacity and the most adopted green energy resource all over the world [1]. In developing countries like India, it has become the most comprehensive form among other types of green energy technology [2]. Photovoltaic cells and solar towers can be adopted for converting solar thermal energy into electricity, while solar collectors can harness thermal energy for medium- and low-temperature engineering applications [3,4]. Solar collectors using air as a working fluid are advantageous because of their simpler construction, ease of maintenance, and minimum investment. Mainly, solar collectors are ideal for simple heating applications [5], including space heating, energy storage [6], crop drying, and dehumidification projects [7]. However, the lower thermal capacity of air and the varying solar radiation are a few notable disadvantages of using solar air collectors [8].

In conventional air heaters, the atmospheric air circulated within the solar collector remains in a viscous laminar flow. It results in a very minimal heat transfer coefficient value of inlet air leading to minimal efficiency of the heater. Researchers have looked into various ways of increasing heat transfer by rupturing the laminar sublayer with turbulence-inducing elements on the base plate to address this issue [9]. It is the most effective approach for creating artificial roughness on the base plate that reduces thermal resistance by disturbing the laminar layer. Introducing fins on the base plate further enhances the heat transfer characteristics [10]. However, the effect comes at the cost of a rise in pumping power through the roughened base plate, which requires additional electrical energy, thereby increasing power consumption. It is thus crucial to evaluate a thermal collector's heat transfer performance and airflow characteristics to create an optimal and effective system. The thermohydraulic augmentation factor is a measure that relates the heat transfer rate within the system to the fluid flow characteristics, which toggles with frictional parameters and pressure drop through the flow chamber [11]. Another method to enhance the operation of a thermal collector under turbulent flow conditions is by utilizing stagnant energy at the inner face of the absorber plate [12]. This stagnant energy is usually not transported by the air due to insufficient time [13]. There are two main techniques for exploiting this energy: The first involves breaking the viscous sublayer, which stores this energy, and creating a geometrical roughness on the plate [14]. The second technique involves impeding and remixing the air to lift it toward the absorber plate to extract energy from the laminar sublayer with the help of turbulators. The second technique, however, results in a substantial enhancement in thermal energy transfer and pressure drop when the roughness is much larger than the thickness of the sublayer. Studies have investigated the properties of flow in rectangular protruded ducts, primarily utilized in thermal collectors, to augment the heat energy transfer from the collector absorber plate and active fluid at lower cost and pumping power [15–17]. Researchers have found that the periodicity of flow rises with the Reynolds Number (Re), and the total loss coefficient develops almost steadily when the resistance to flow is high [18].

Several authors have researched the augmentation of solar thermal collectors' thermal characteristics. Li et al. [19] performed an empirical study on the fluid flow's mean velocity, pressure drop, and turbulence around baffles for the Re varying between 600 and 10,500. Their results showed that as Re increased, the flow became periodic after crossing two to five baffles, and the total loss coefficient remained relatively constant when the pressure drop ratio was high. Habib et al. [20] placed baffles with a unique shape on the two parallel heating surfaces and achieved an improved heat transfer while maintaining a constant wall flux on the test plate surfaces. They found that enhancing the Re, choosing higher thermal conductivity material for the baffle, and minimizing the space between them resulted in an average heat transfer coefficient value. However, further study revealed that the average heat transfer and pressure drop factors improved while increasing the baffle height and flow velocity [21]. A significant increase in pressure loss was observed when comparing the pressure drop and average thermal energy transfer rate. Liou et al. [22] reported an in-depth experimentation on the solar collector's turbulent heat transfer for the Re varying from 5.103 to 54.103 in another study. Typically, the solar collector duct is a rectangular shape having ribs to stimulate the turbulent flow inside the collector. Their research demonstrated increased heat exchange at the cost of a significantly higher-pressure loss.

The main goal of this research is to augment the efficiency of thermal energy transfer between the absorber plate and working fluid while prioritizing system lightweight, durability, and minimum pumping power consumption. In the present work, to achieve this, a novel carbon nanotube (CNT) pin fin and turbulators are tested in a conventional solar air collector. The CNT pin fins intend to increase the base plate surface area subjected to the inlet airflow. At the same time, the turbulators break the laminar boundary layer and form the vortex effect phenomena near the turbulator region. The study depicts how this enhanced the useful heat transfer from the absorber plate to inlet air.

2. CFD Modelling

Computational fluid dynamics (CFD) modelling is used as a tool to carry out numerical methods and algorithms to simulate and analyze the behaviour of fluids, their interaction with their surroundings, and other aspects of the system without its physical realization. The method is employed considering its potential to save time and resources by reducing the number of costly and time-consuming trials. This manuscript aims to implement the aforementioned idea in solar collectors through CFD modelling. It will include an overview of the parameters, boundary conditions, and solver settings used in the modelling carried out in the work.

2.1. Solar Thermal Collector Parameters

A smooth conventional solar air collector geometry with dimensions 2000 mm × 1000 mm × 70 mm is shown in Figure 1 [23,24]. The base absorber is a rectangular plate made of a 2 mm thick aluminium sheet and a glass cover sheet with 3 mm in thickness resting at a height of 50 mm above the collector plate, firmly supported by the wooden structure. The wooden box accommodates the aluminium absorber plate, glass plate, and duct provisions to facilitate airflow. The inlet portion of the duct is a 100 mm long pipe with a 50 mm diameter, and the outlet portion of the duct is a 100 mm long pipe with a 25 mm diameter. The wooden box has 1 cm of thick glass wool for insulation [25,26].

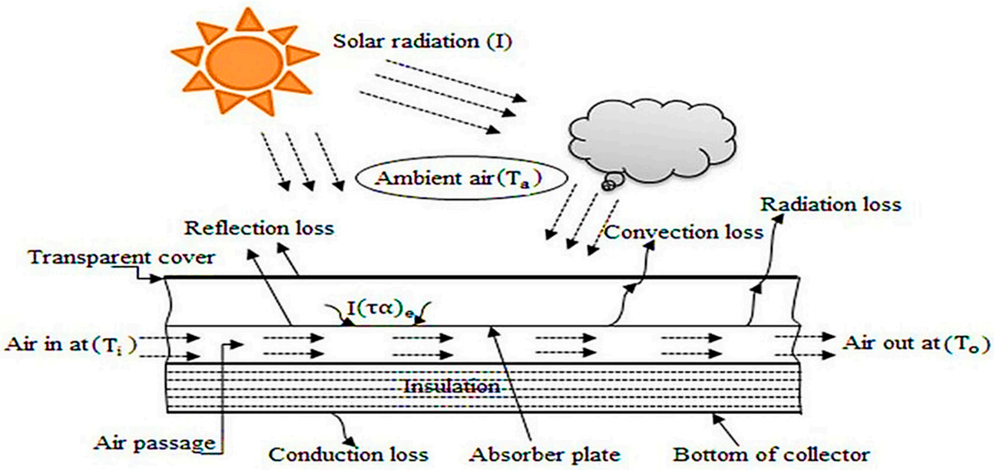

Figure 1. Basic solar thermal collector.

2.2. Governing Equations

The simulation has adopted the RNG k-ε model to provide an accurate representation of the turbulent flow field. On the other hand, the Nusselt equation (Equation (1)) is another primary equation used to represent a band of attributes from convective heat transfer to the thermal conductivity of the fluid. The Reynolds number describes the nature of flow as laminar or turbulent, which is given in Equation (2). The other fundamental equations used to predict fluid flow include the continuity, momentum, energy, and flow turbulence models, depicted in Equations (3)–(7).

$$\text{Nu} = \frac{h\ D_h}{K_{eff}} \tag{1}$$

$$\text{Re} = \frac{U\ D_h}{\nu} \tag{2}$$

Continuity equation:

$$\nabla \cdot \left(\rho \cdot \vec{v} \right) = 0 \tag{3}$$

Momentum equation:

$$\nabla \cdot \left(\rho \cdot \vec{v} \cdot \vec{v}\right) = -\nabla_\rho + \nabla \cdot \left(\mu \left[\left(\nabla \vec{v} + \nabla \vec{v}^T\right) - \frac{2}{3} \nabla \cdot \vec{v} I\right]\right) + \rho \vec{g} \tag{4}$$

Energy equation:

$$\nabla \cdot \left(\vec{v}(\rho E + p)\right) = \nabla \cdot \left(K_{eff} \nabla T - h\vec{J} + \left(\mu \left[\left(\nabla \vec{v} + \nabla \vec{v}^T\right) - \frac{2}{3} \nabla \cdot \vec{v} I\right] \cdot \vec{v}\right)\right) \tag{5}$$

where, K_{eff} is the effective conductivity.

The fluid turbulence model is calculated using the following transport equations.

$$\frac{\partial}{\partial x_i}(\rho k u_i) = \frac{\partial}{\partial x_j}\left(\alpha_k \mu \frac{\partial k}{\partial x_j}\right) + G_k + G_b - \rho\varepsilon - Y_M + S_k \tag{6}$$

$$\frac{\partial}{\partial x_i}(\rho \varepsilon u_i) = \frac{\partial}{\partial x_j}\left(\alpha_\varepsilon \mu \frac{\partial \varepsilon}{\partial x_j}\right) + C_{1\varepsilon} \frac{\varepsilon}{k}(G_k + G_{3\varepsilon} G_b) - C_{2\varepsilon}\rho \frac{\varepsilon^2}{k} + S_\varepsilon \tag{7}$$

where, $C_{1\varepsilon}$ and $C_{2\varepsilon}$ are the model constants that have the finite value of 1.42 and 1.68, respectively, and k is the turbulence kinetic energy.

Table 1 provides the individual thermal properties of the solar collector components required for the numerical assessment.

$$\rho = 3.915 - 0.01608\, T + 2.901 \times 10^{-5} T^2 - 1.941 \times 10^{-8} T^3 \tag{8}$$

$$K_{eff} = \left(0.001521 + 0.0975\, T - 3.332 \times 10^{-5} T^2\right) \times 10^{-3} \tag{9}$$

$$\mu = \left(1.616 + 0.0652\, T - 3.029 \times 10^{-5} T^2\right) \times 10^{-6} \tag{10}$$

Table 1. Thermal properties of the solar collector components.

Materials	Density	Thermal Conductivity	Specific Heat	Viscosity
	(kg/m^3)	**(W/mK)**	**(J/kg.K)**	**(kg/ms)**
Air	Equation (8)	Equation (9)	1006.34	Equation (10)
Glass cover	2500	1.2	800	-
Aluminium	2719	202.4	871	-
CNT	1740	3000	570	-

2.3. Performance Parameters

Since the CFD models are required to be compared against theoretical value, it is essential to establish the performance parameter as a reference base prior to the CFD modelling. Instantaneous thermal efficiency (η_t) and pumping power consumption (ΔP) are the two key parameters used to benchmark the performance of the modelled system. They are theoretically calculated from Equations (11) and (12) and are used to know the characteristics of the solar thermal air collector under different boundary conditions.

$$\eta_t = \frac{Q_u}{I_T A_p} \times 100 \tag{11}$$

$$Q_p = \frac{\dot{m}}{\rho}\ \Delta P \tag{12}$$

2.4. Boundary Conditions and Solver Settings

Several typical experimental conditions are given as boundary conditions in the ANSYS Fluent module for performing the numerical simulation in a solar thermal collector. The collector tilt angle must be perpendicular to the incoming solar radiations. And so, the latitude angle is taken as the collector tilt angle. The air's inlet temperature and mass flow rate are assumed to be uniform throughout the simulation. The heat losses from the collector are constantly varied, which mainly depends upon the collector surface temperature. The properties of the circulating air are varied with respect to temperature; the empirical equation for this thermal property is loaded in the fluent material properties. The base plate is set as a wall boundary condition where solar irradiance is given as heat flux. The solar irradiance is multiplied with an absorptivity value of 0.95 to consider reflection losses from the collector bottom surface. The collector side is set as a wall in ANSYS Fluent boundary conditions, in which the heat is rejected from the thermal collector to the atmosphere. The equivalent velocity inlet condition to the concerned Re is applied perpendicular to the inlet duct, with a fixed temperature of 303 K at the inlet. Pressure flow outlet boundary conditions are set as a backward pressure of 0 Pa applied at the outlet duct. The net transmissivity of the glass plate is taken as 0.95, where the boundary conditions are set as the heat is rejected from the glass cover to the ambient conditions. The fluid velocity for the corresponding Re varies from 3000 to 15,000 in steps of 1500, resulting in nine numerical simulations per model. The boundary conditions applied to the numerical model simulation are represented in Table 2. CFD simulations involve solving a set of partial differential equations (PDEs) that discuss the behaviour of the fluid flow. Solver settings play a critical role in CFD simulations as they determine how fluid flow equations are solved, thereby impacting the simulation's accuracy, efficiency, and stability. The simulation utilizes the following solver settings:

- The SIMPLE scheme is adopted to calculate the flow problem. This method couples the velocity and pressure corrections to apply mass conservation in order to calculate the pressure field;
- The residual values are set to a threshold of below 10^{-6} to achieve convergence in the solution;
- The pressure is formulated using the weighted body force method.

Table 2. Boundary conditions for the numerical simulation.

Parameters	Boundary Condition
Absorber top surface	Wall
Glass cover	Wall
Absorber side	Wall
Air inlet	Velocity inlet
Air outlet	Pressure outlet
Residuals	10^{-6}

2.5. Grid Impedance Test

To confirm that the solutions attained are not dependent on the number of mesh elements used, a test was performed by augmenting the number of elements in the mesh by minimizing the size of each element. The Nusselt number (Nu) of the heat transfer in the absorber plate was correlated between the different mesh configurations. This analysis was conducted to confirm the accuracy of the CFD code used. Here, the simulation was carried out for 0.02157 kg/s mass flow rate for a Re of 12,000. A mesh of 0.87 million elements was used as the standard for the numerical analysis of the base model due to the requirement of numerous numerical simulations and limitations in the computational speed. Figure 2 shows the resulting Nu for varying mesh sizes. For the absorber plate with CNT pin fin configuration, a mesh of 0.94 million elements was used in the simulation.

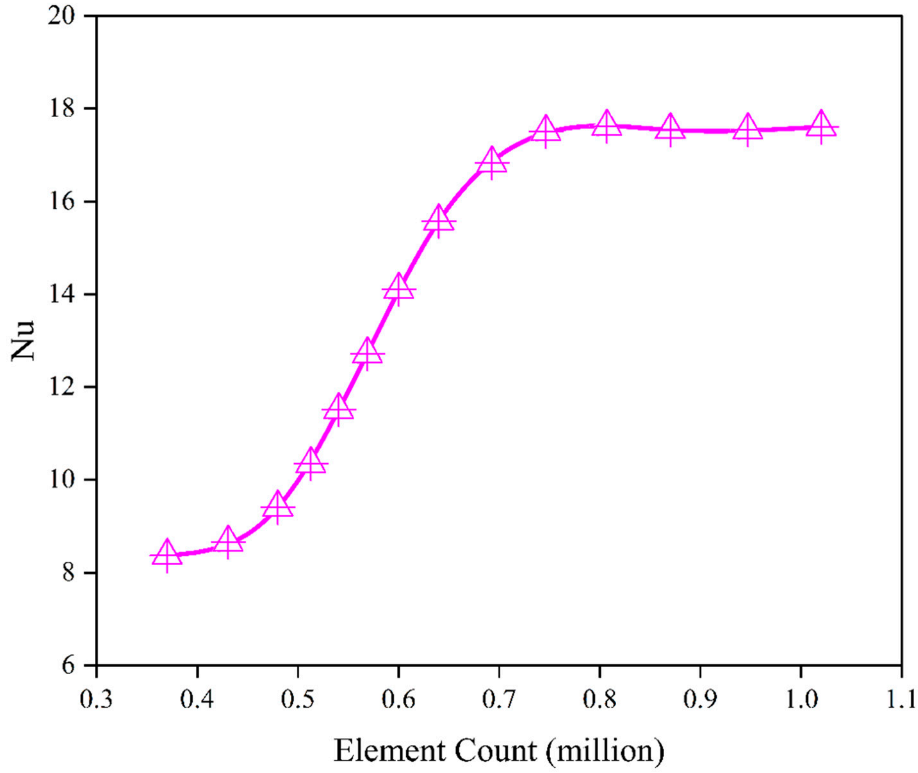

Figure 2. Variation in the Nu while varying the mesh size.

3. Results and Discussion

To study the proposed CFD model, it is important first to identify the model that would produce the most accurate result. For this purpose, a simulation of the current solar thermal collector was tested using three turbulence models: the Renormalisation Group (RNG) k-ε model, the Standard k-ω model, and the Standard k-ε model. The results obtained from the three different models were then compared to theoretical Nu values. Figure 3 shows the numerical comparison results obtained from the three different models as opposed to the theoretical values. The graph clearly illustrates that compared to the other models, the RNG k-model's numerical values were closer to the theoretical Nu values. As a result, the RNG k-model was chosen for numerical simulations henceforth. It is worth noting that this decision was important in ensuring that the results obtained from the simulations carried out in the proposed model were accurate and reliable. Additionally, several other authors recommended the same turbulence model for the simulation of solar thermal collectors [27,28]. After choosing the right turbulence model, three simulations were carried out: collectors with CNT pin fins, collectors with turbulator, and collectors with both CNT pin fins and turbulators.

3.1. Effect of CNT Pin Fin Models with Different Heights

The pin fins, each having a diameter of 30 mm, were strategically placed atop the flat plate collector in a configuration consisting of 5 rows and 15 columns. This innovative arrangement was entirely integrated into the fluid flow channel, augmenting the absorber plate's surface area exposed to the air stream. Notably, the addition of pin fins served to curtail the hydraulic diameter of the airflow duct, resulting in heightened thermal energy transfer from the duct to the inlet airflow. Furthermore, it must be emphasized that the hydraulic diameter was inversely proportional to the plate heat transfer coefficient. Thus, the plate heat transfer coefficient was simultaneously increased by decreasing the hydraulic diameter. It is interesting to note that, in this investigation, the pin fin material employed was the novel material CNT. Figure 4 illustrates the solar collector outfitted with the proposed pin fin arrangement, and Figure 5 represents the 3D representation of a section of the proposed collector.

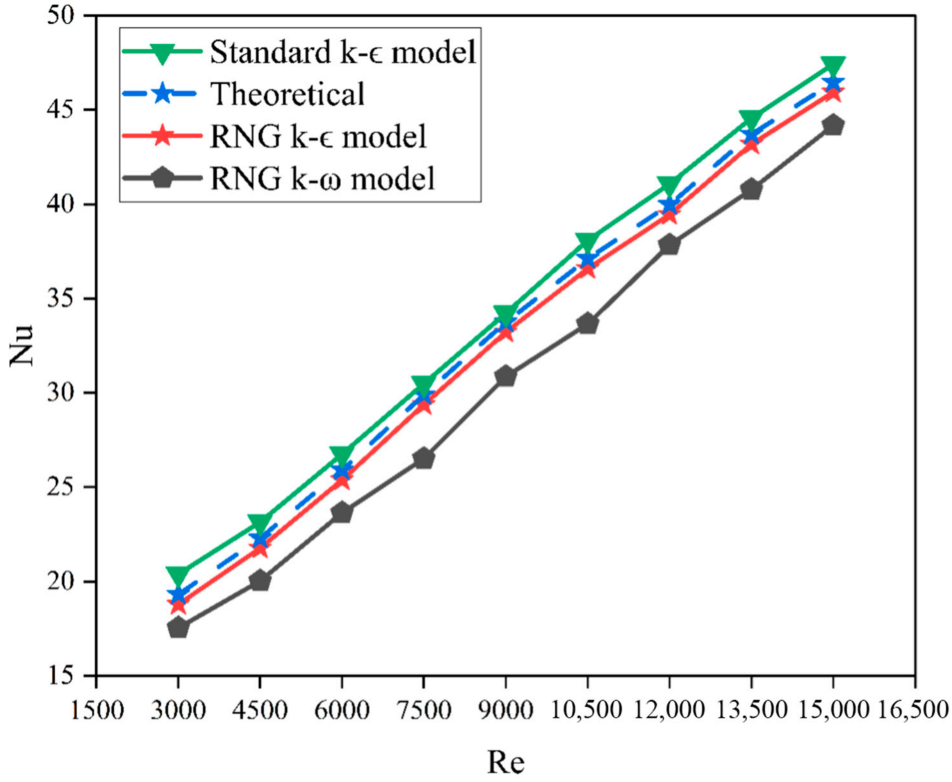

Figure 3. Comparison of Nu values for various Re values from the different turbulence models and theoretical calculation.

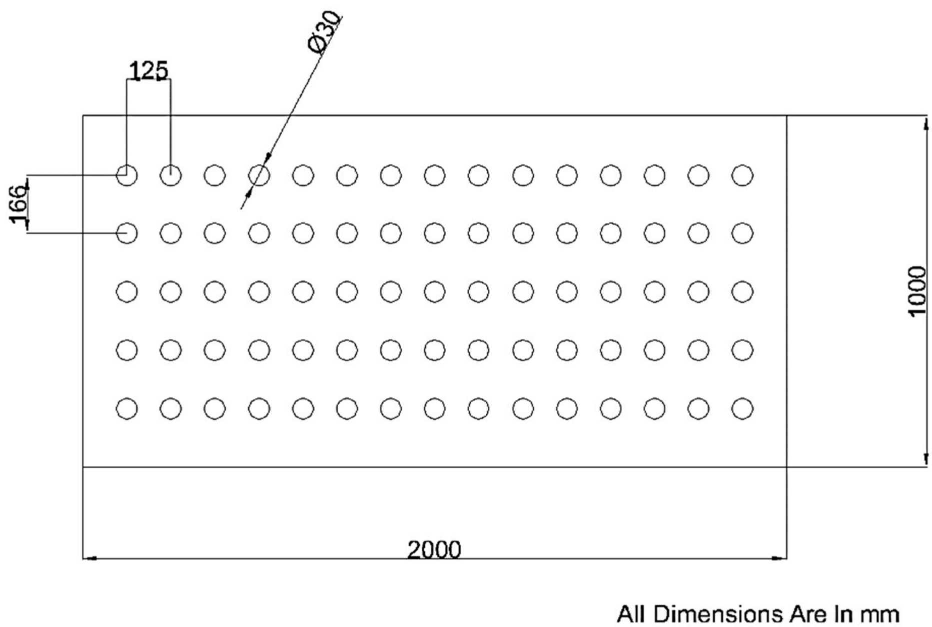

Figure 4. 2D representation of the entire section of a solar collector with pin fins and their dimensions.

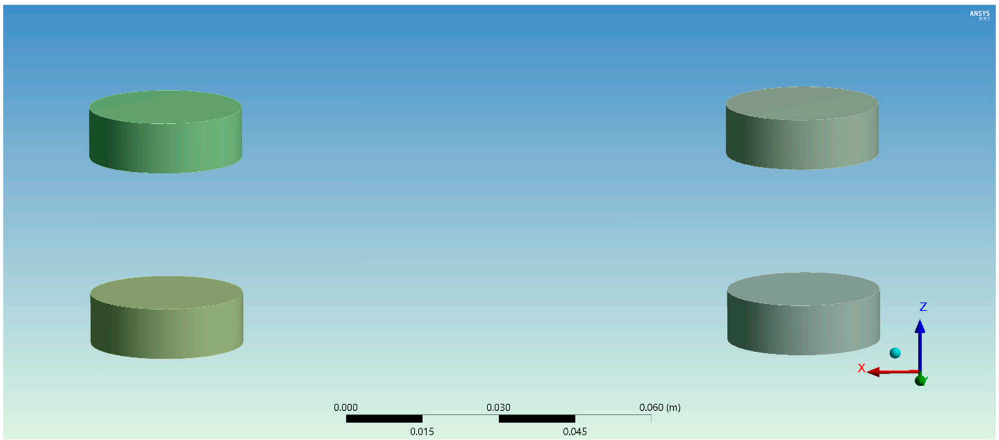

Figure 5. 3D representation of a section of a solar collector with pin fins.

CNTs are a promising material for improving the thermal behaviour of solar collectors due to their unique properties. As fins, they offer advantages over traditional metal fins, including high thermal conductivity, low weight, and high aspect ratio. It is required to mention that it is possible to use CNT material to fabricate the designed pin fin [29]. Using CNT-based straight fins in solar collectors has indeed been shown to enhance the heat transfer coefficient and augment overall efficiency. The exceptional thermal conductivity of CNTs allows efficient heat transfer between the collector duct and the airflow [30]. Incorporating CNTs as fins diminishes the hydraulic diameter of the collector, amplifying the heat energy transfer rate. With their lightweight nature, CNTs prove to be an optimal choice for hassle-free installation and transportation. At the same time, their high aspect ratio furnishes a generous surface area for heat transfer, elevating the collector's efficiency to new heights.

Numerical simulations were conducted on a solar thermal collector with pin fins at a different Re. At a higher Re, the inertia force of the airflow dominated over the viscous force. Clear visualization of the air streamlines across the pin fin is shown in Figure 6. This effect reduces the friction factor for the working fluid flow. From the results, the temperature contour of the collector integrated with pin fins is presented in Figure 7. The numerical results show a decrease in the Nu of the fluid flow. The flow in the smooth duct remained undisturbed, with parallel streamlines indicating minimal turbulence. Consequently, the mixing of fluid layers was reduced, resulting in relatively lower Nu compared to the modified plates. Figure 8 illustrates the velocity contour front view of the airflow stream, and Figure 9 shows the top view representing the velocity variation across the stream.

However, the introduction of pin fins caused the formation of vortices and flow separation downstream, leading to increased turbulence and mixing of fluid layers. In Figure 10, the airflow separation across the pin fin is depicted. High-temperature spots were detected downstream of the fins. It is likely due to the separation of laminar regions, resulting in a low heat transfer in those areas [31]. Although the flow separation reduced heat transfer from the absorber surface to the circulating air, the vortices created attachment and detachment points, enhancing overall heat transfer. This effect is evident in the numerical results presented in Figure 11. The Nusselt number of a flat plate with 30 mm CNT pin fins is 113.05 at Re = 15,000, which is 176% higher than the collectors without modifications. The Nu ratio for various Re is illustrated in Figure 12. This effect was more significant under higher turbulent flow conditions, where the Re of the flowing fluid enhanced, and the turbulent effects dominated over secondary flow.

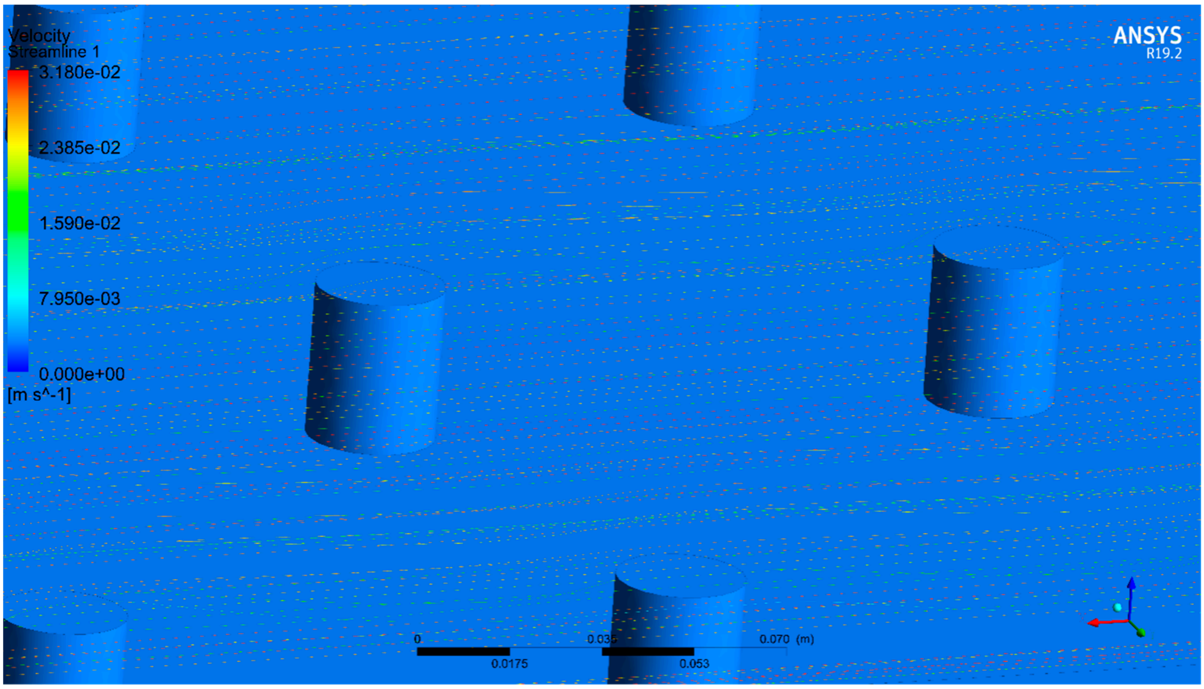

Figure 6. Air velocity streamlines over the pin fin.

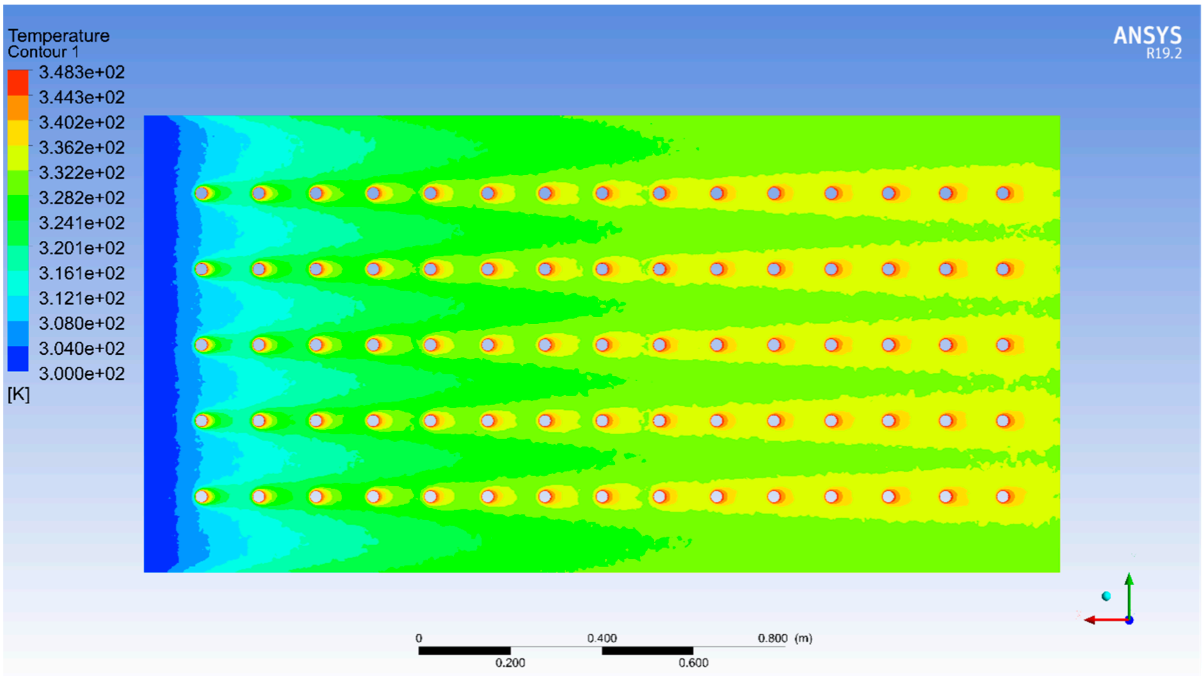

Figure 7. Temperature contour at a distance of 20 mm from the bottom base plate.

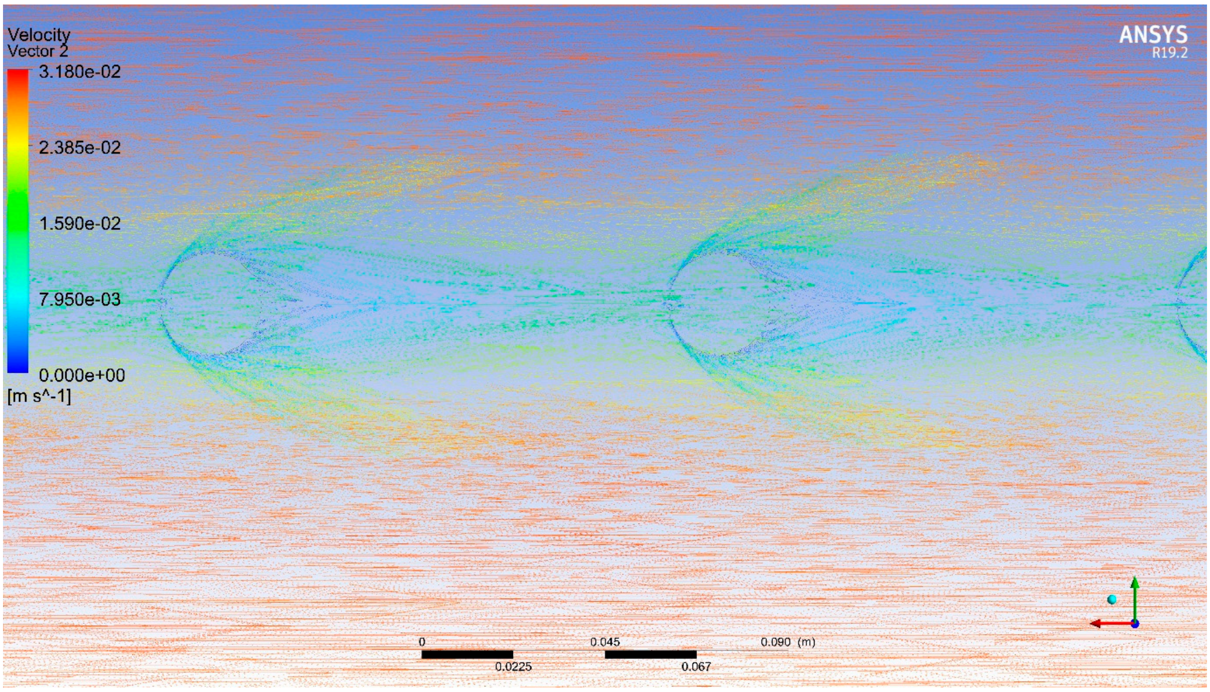

Figure 8. Air velocity variation across pin fin.

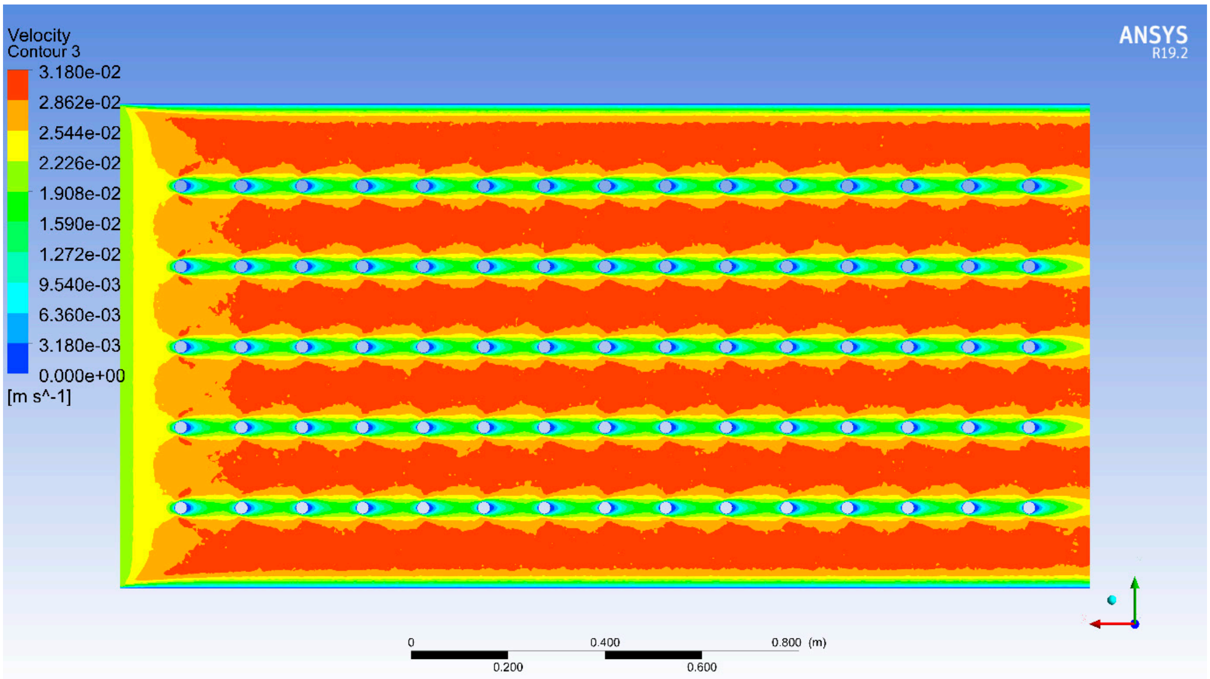

Figure 9. Velocity contour at a distance of 20 mm from the bottom base plate.

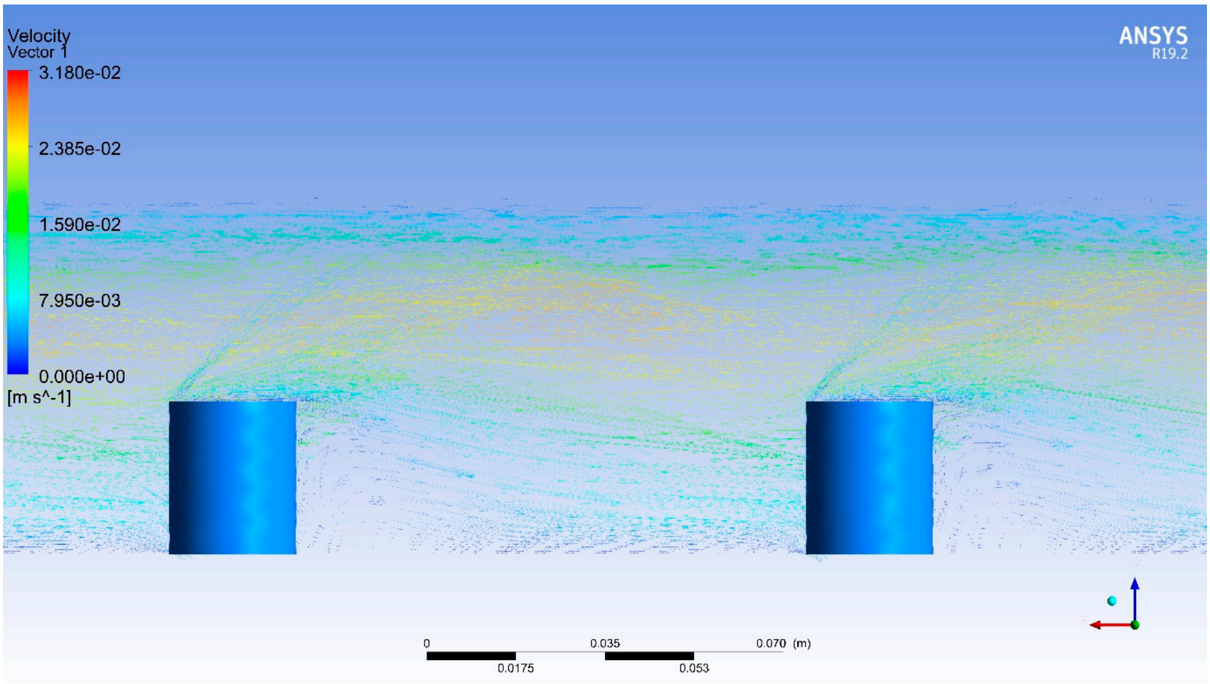

Figure 10. Air turbulence due to pin fin arrangements.

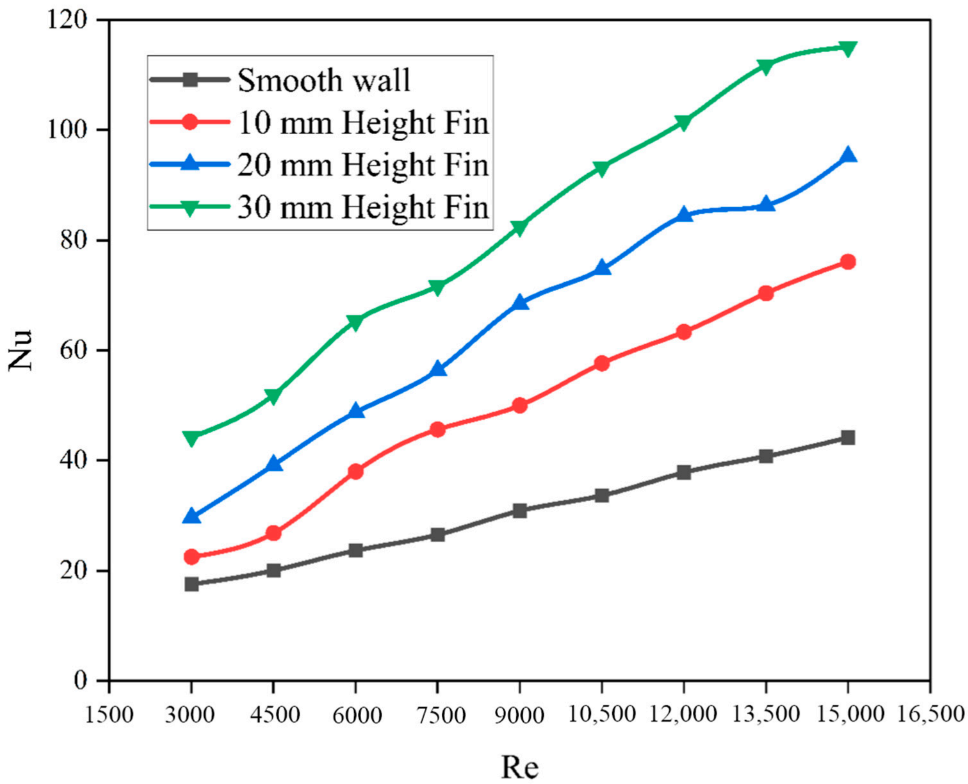

Figure 11. Effect of Re on solar collector's Nu.

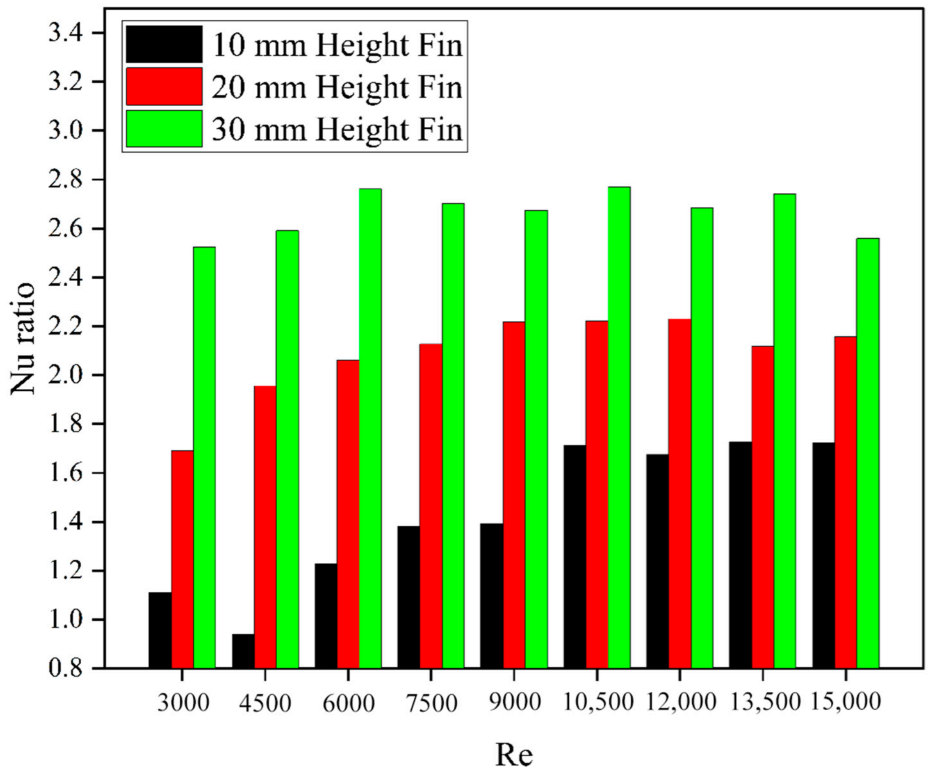

Figure 12. The Nu ratio for various Re.

3.2. Effect of Different Heights in CNT Turbulator Model

CNT turbulators have been found to significantly enhance the efficiency of thermal air heaters by effectively disrupting the flow sublayer. The flow pattern of the turbulators closely resembles that of continuous fins, except for the area near the fins and grooves [32]. The streamlines in the continuous fins were closer to the rib portion, indicating a higher flow rate than the turbulators. However, the groove cavities of the CNT turbulators exhibited an increase in fluid flow separation and vortex development, resulting in a decrease in turbulence intensity and kinetic energy within a minor area of the grooves. It affects the heat exchange between the base plate and the inlet air, influenced by the net result of fluid flow separation and vortex development in the vicinity of the rib area. The Nusselt number of a flat plate with 30 mm CNT turbulators is 85.03 at Re = 15,000, which is 122% higher than the collectors without modifications. Despite the use of CNT turbulators, the Nu remains almost the same or is slightly reduced at various Re compared to continuous fins. Figure 13 denotes a solar collector with turbulators, and Figure 14 illustrates the 3D representation of a section of the proposed collector.

Despite having a higher wall temperature of the base plate, the smooth duct resulted in a lower Nu than ducts with extended surfaces. Interestingly, the exit air temperature seemed to be lower at a certain distance from the wall surface. However, both turbulators exhibited an augment of thermal energy being absorbed by the inlet air from the duct wall surface due to the occurrence of laminar flow breakage elements, resulting in a highly increased Nu. Improvement in heat exchange was also observed in the hot spots, which were smaller in the turbulators than in the fins, indicating greater flow separation. This improvement could be attributed to a small amount of air trapped inside the cavity areas, leading to bursts of heat retention in that volume. The number of turbulators and the heat retention inside the cavities influenced the heat transfer rate. Figure 15 illustrates the Re’s impact on the solar collector’s Nu for various Re. Figure 16 shows the Nu ratio of turbulators at different Re. The results indicate turbulators led to a slightly lower Nu than fins across different Re. These observations are in agreement with the data on turbulence kinetic energy and the contour patterns of streamlines.

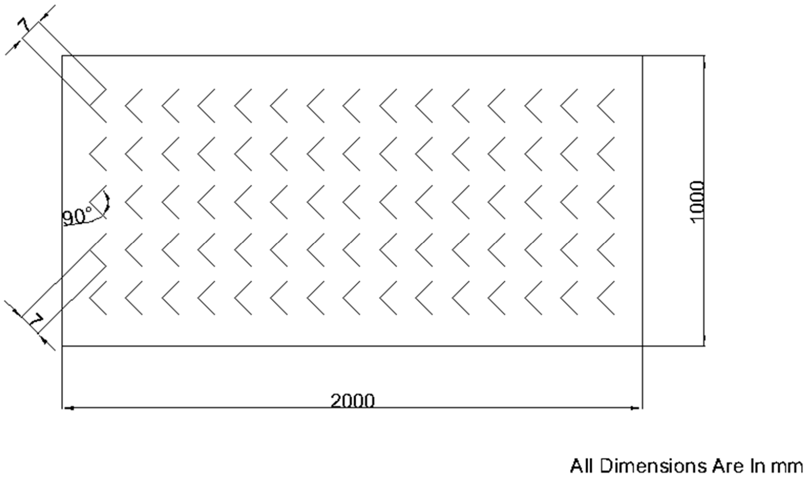

Figure 13. 2D representation of the entire section of a solar collector with turbulators and their dimensions.

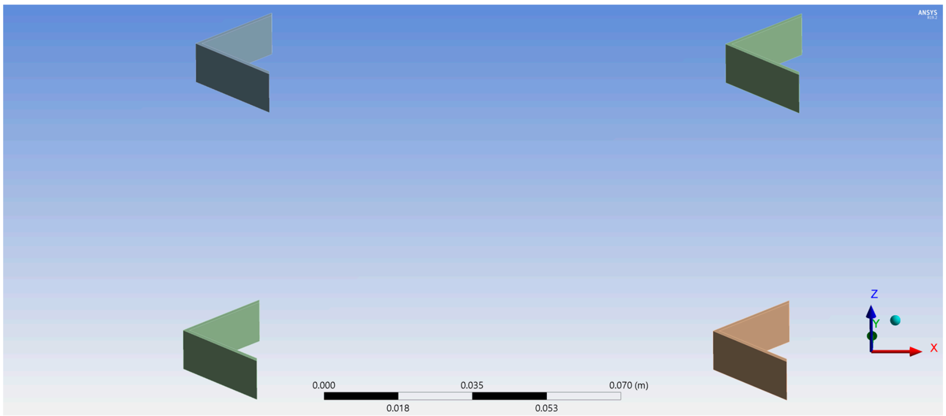

Figure 14. 3D representation of a section of a solar collector with turbulators.

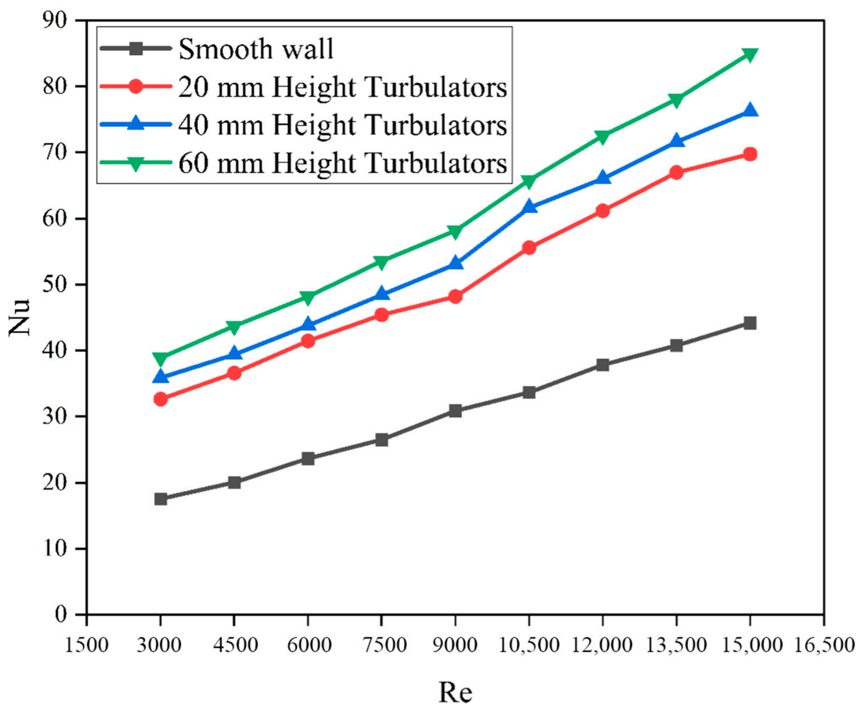

Figure 15. Influence of Re on solar collector's Nu.

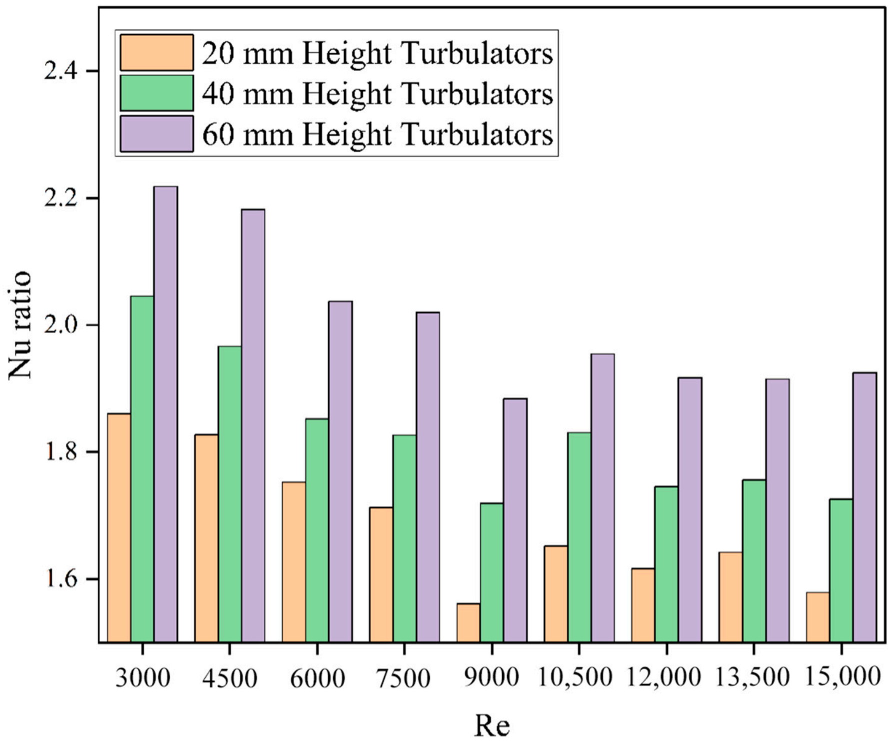

Figure 16. The Nu ratio for various Re.

3.3. Effect of Different Heights of CNT Pin Fins and Turbulators

A numerical assessment was conducted using three different diameters of CNT pin fins (h), three different heights of the turbulator (H), and nine Reynolds numbers (Re) varying from 3000 to 15,000. The best values of h, H, and Re were determined through the numerical analysis, and complete specifications of the analysis are provided in Table 3. Figure 17 illustrates the solar collector with both pin fins and turbulators, and Figure 18 denotes the 3D representation of a section of the proposed collector.

Table 3. Simulation parameters to find optimal conditions.

Run	Pin Fin Height (mm)	Turbulator Height (mm)
1	10	20
2	20	20
3	30	20
4	10	40
5	20	40
6	30	40
7	10	60
8	20	60
9	30	60

The conventional solar collector thermal efficiency can be enhanced by incorporating passive heat transfer techniques such as CNT pin fins and turbulators. They increase heat transfer by promoting fluid mixing and disrupting the laminar boundary layer. Fins, which are extended surfaces protruding into the flow, are commonly used to improve heat transfer in various heat transfer devices. In solar air collectors, fins are typically attached to the base plate, increasing the surface area exposed to heat transfer. This increase in surface area can lead to better heat transfer rates and thus augment the overall efficiency of the solar air collector. Pin fins can be used to be straight or curved and can be spaced at varying distances from each other, depending on the specific application. However, closely spaced pin fins can cause more flow resistance, leading to an increased pressure drop across the collector.

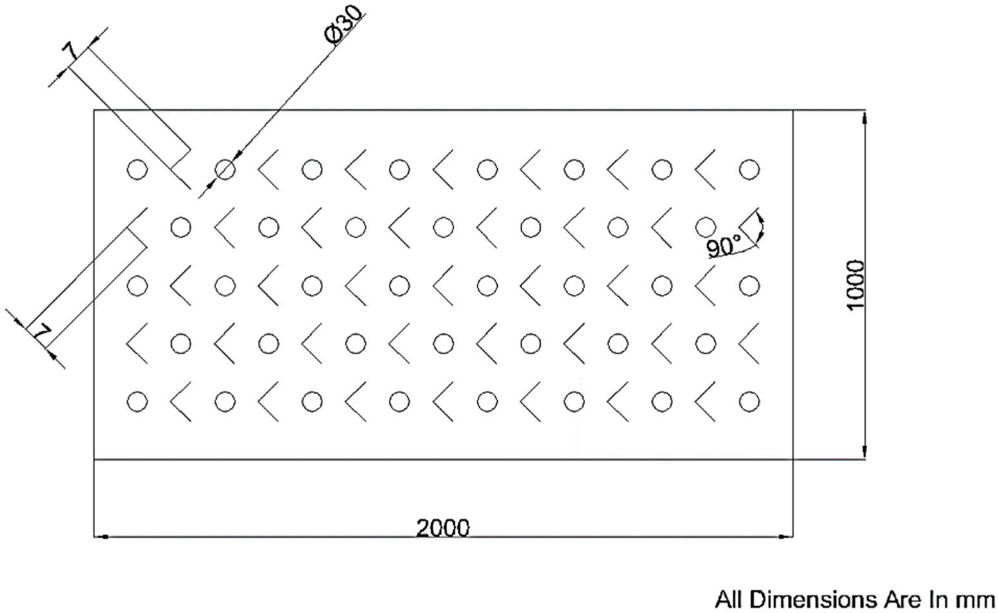

Figure 17. 2D representation of the entire section of a solar collector with pin fins and turbulators and their dimensions.

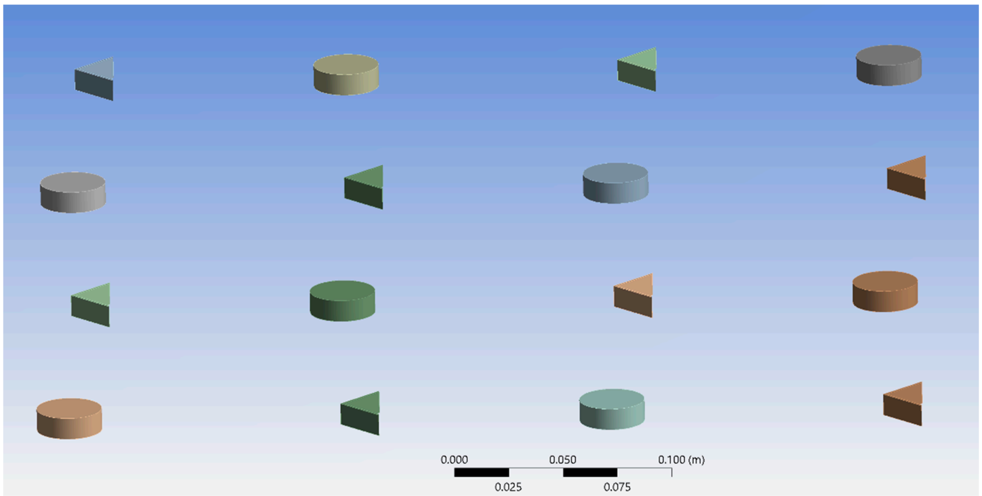

Figure 18. 3D representation of a section of a solar collector with pin fins and turbulators.

Turbulators are another passive heat transfer enhancement technique that can be utilized to improve heat transfer in solar collectors. They are essentially small obstacles that are placed within the flow channel to induce turbulent flow, which can increase the velocity of the fluid and promote mixing, leading to better heat transfer rates. In solar air collectors, turbulators are typically designed as small ridges or bumps on the base plate, which can cause the airflow to break into smaller eddies. Compared to pin fins, turbulators are often more effective in promoting heat transfer, especially under turbulent flow conditions. Figure 19 illustrates the Nu ratio for various pin fin heights and turbulator designs. The Nusselt number of a flat plate with 20 mm CNT pin fins and 40 mm turbulators is 137.37 at Re = 15,000, which is 211% higher than the collectors without modifications. In this condition, the efficiency of the thermal collector is found to be 89.54%.

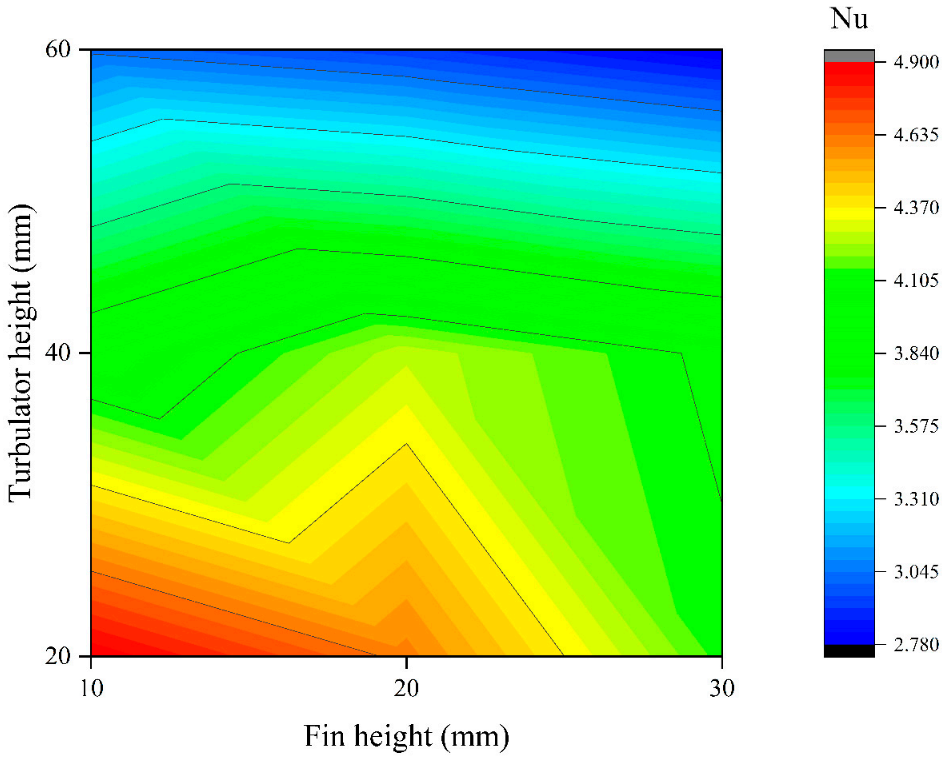

Figure 19. Nu ratio for various CNT pin fin heights and turbulators.

The effect of fins and turbulators on solar air collector performance is based on the collector geometry, flow conditions, and design of the fins or turbulators. Figure 20 displays the results obtained from the numerical analysis of the combined effect of fins and turbulators. Solar collector performance is limited under uniform flow conditions, and the introduction of fins disrupts the fluid flow layer, inducing turbulence and improving heat transfer. The Re of the fluid is a crucial parameter that determines the onset of turbulent flow, with a higher Re resulting in more significant enhancements in heat transfer. These passive techniques are important for improving the efficiency of solar collectors.

Integrating carbon nanotube (CNT) pin fins and turbulators in solar flat plate collectors can potentially revolutionize their performance and efficiency. Carbon nanotubes, known for their exceptional thermal and mechanical properties, offer unique advantages when applied to heat transfer systems.

CNT pin fins, similar to conventional pin fins, are small protrusions attached to the base plate of a thermal collector. However, their incorporation with carbon nanotubes introduces several significant enhancements. The excellent thermal conductivity of CNT allows them to efficiently conduct and transfer heat from the base plate to the working fluid, leading to improved heat transfer rates and enhanced overall thermal efficiency of the collector.

In addition to their high thermal conductivity, CNT pin fins also exhibit a large surface-area-to-volume ratio. This property increases the contact surface area between the absorber plate and the air, facilitating a more efficient heat energy transfer.

Moreover, CNT pin fins offer superior mechanical strength and structural stability, allowing them to withstand high temperatures and pressures without deformations or failures, ensuring their long-term functionality and durability in solar flat plate collectors.

Similarly, integrating CNT turbulators within the fluid flow channels of the collector brings significant improvements. CNT turbulators enhance the turbulence of the fluid flow, leading to increased convective heat transfer. The turbulent flow disrupts the laminar boundary layer and promotes better mixing, resulting in a more effective heat transfer. The enhanced convective heat transfer coefficient achieved with CNT turbulators significantly improves the overall efficiency of the collector.

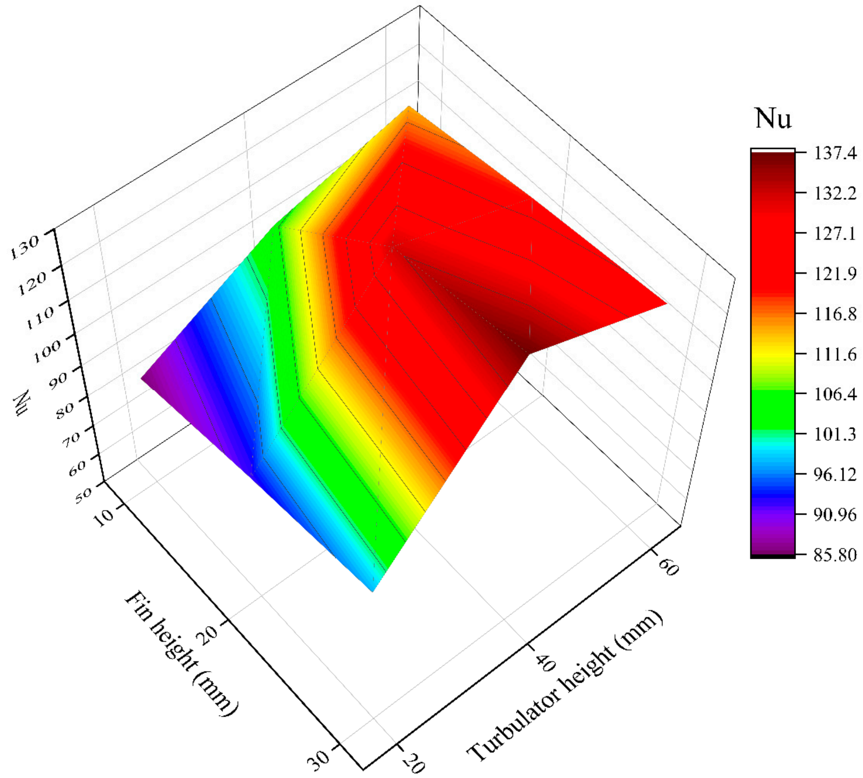

Figure 20. Effect of fins and turbulators on solar collector's Nu.

Furthermore, carbon nanotubes possess unique optical properties, such as high light absorption and low reflectance, allowing them to absorb solar radiation efficiently and maximizing the utilization of incoming sunlight. By absorbing a greater amount of solar energy, the collector equipped with CNT pin fins and turbulators can achieve higher thermal outputs and increase its overall energy conversion efficiency.

Their incorporation results in a more uniform temperature distribution across the absorber plate by promoting fluid mixing while simultaneously disrupting the boundary layer, thereby reducing temperature gradients and minimizing heat losses. This optimization of heat gain further augments the overall performance of the collector.

Furthermore, the exceptional mechanical strength and durability of carbon nanotubes contribute to the long-term reliability and robustness of the entire collector system. Their high-temperature stability allows for sustained performance even under harsh operating conditions.

The integration of CNT pin fins and turbulators in solar flat plate collectors offers substantial improvements in their competence and carries the potential to revolutionize the field of solar thermal energy utilization and contribute to the advancement of sustainable energy solutions.

Thus, the results show that using fins and turbulators in solar collectors can enhance the heat transfer process by promoting fluid mixing and disrupting the boundary layer. The performance of these passive heat transfer techniques is influenced by turbulator area, height, fin height, and fin pitch. A fin height of 20 mm and turbulator height of 40 mm represent an optimal design amongst the tested combinations that showcase the significantly improved performance of solar air collectors, resulting in increased energy savings and reduced environmental impact.

3.4. Effect of Different Heights of CNT Pin Fin and Turbulator Model on Pressure Drop

The implementation of pin fins and turbulators in solar flat plate collectors enhances the flow resistance leading to a pressure drop across the thermal collector. Generally, pin fins and turbulators are commonly used to augment heat transfer and improve the overall efficiency of solar collectors. Still, they can also impact the flow characteristics within the collector.

Pin fins are small protrusions or extended surfaces attached to the base plate. They increase the surface area exposed to sun rays, promoting better heat absorption and transfer to the working fluid. However, the presence of pin fins also introduces additional flow resistance. The pin fins' geometry, size, and distribution determine the flow resistance. A higher fin density and longer fin lengths generally result in increased flow resistance, leading to higher pressure losses within the collector.

Turbulators, on the other hand, are devices or structures that disrupt the flow and enhance the mixing of the working fluid. They are designed to create turbulence and improve convective heat transfer. Turbulators can be in the form of ribbed surfaces, twisted tapes, or other flow-inducing elements. While turbulators enhance heat transfer, they also increase the collector's flow resistance and pressure loss. Figure 21 denotes the pressure drop due to the effect of fins and turbulators. While comparing the individual effect of pin fins and turbulators in a solar collector, the implementation of both pin fins and turbulators performs well. In addition, solar collectors having a fin height of 20 mm and turbulator height of 40 mm have a superior performance. Also, the efficiency of this collector is varied on different mass flow rates of the air. Figure 22 shows the collector's thermal efficiency with a 20 mm pin fin and 40 mm turbulator under different mass flow rates. On a higher mass flow rate of 0.96915 kg/s (3.49 m^3/h), the thermal efficiency is higher, around 89.57%.

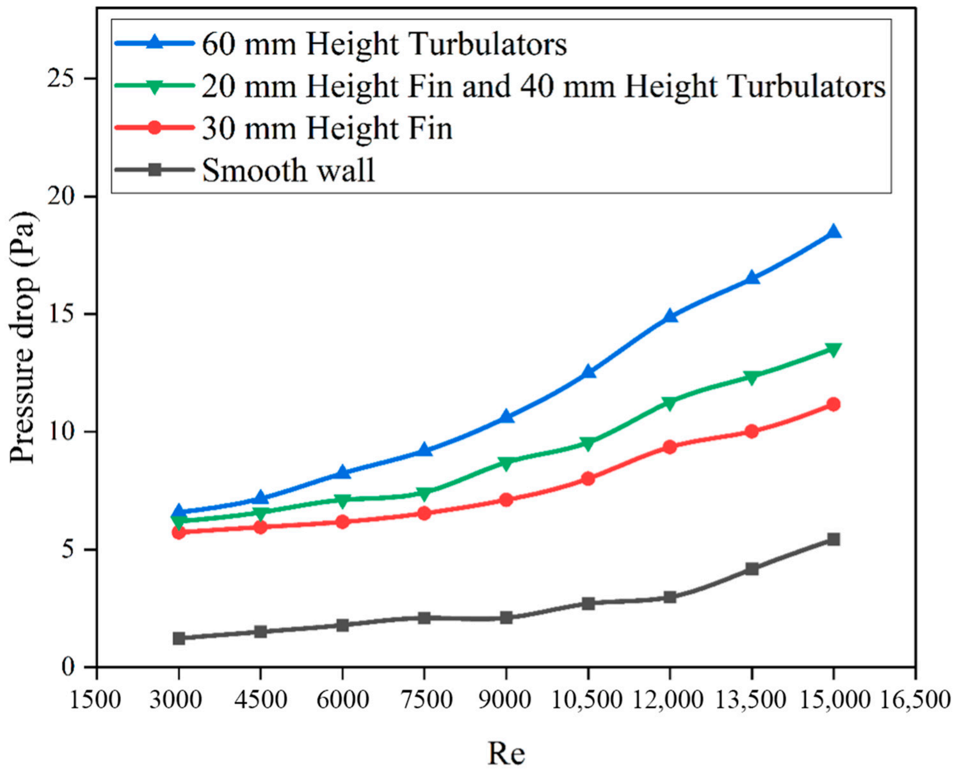

Figure 21. Pressure drop due to the effect of fins and turbulators.

The presence of pin fins and turbulators alters the flow behaviour within the collector, leading to changes in velocity, turbulence, and pressure distribution. The increased flow resistance and pressure loss associated with pin fins and turbulators can affect the pumping power required to circulate the fluid, which in turn impacts the overall system efficiency. Considering these factors during the design of solar flat plate collectors is crucial to ensure optimum heat transfer enhancement while maintaining acceptable pressure losses.

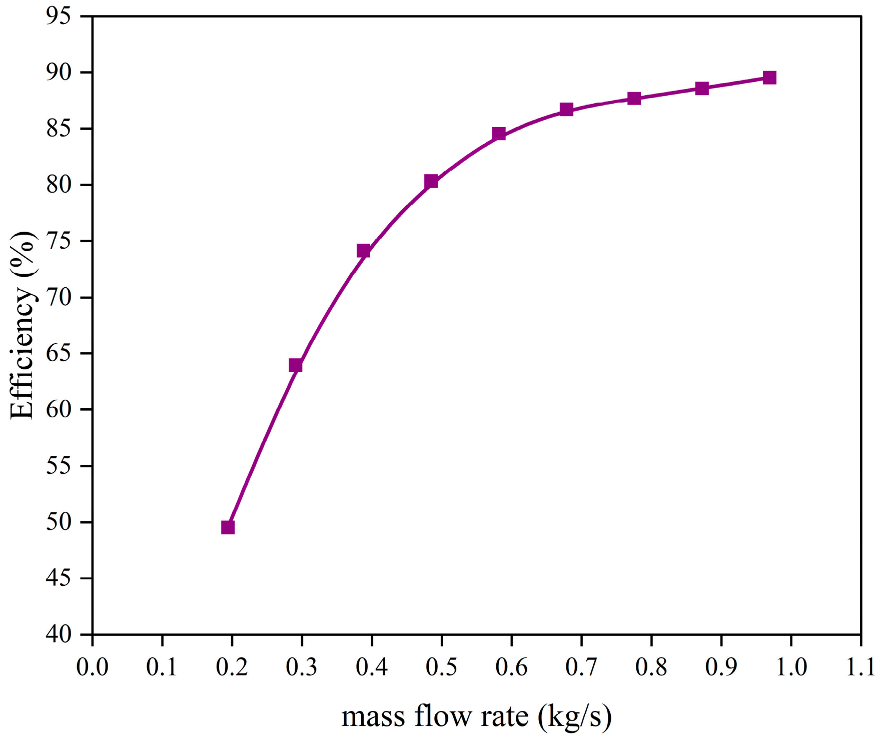

Figure 22. Mass flow rate vs. efficiency of the solar collector having fins and turbulators.

4. Comparative Analysis

The present section compares the results of similar works from the literature with the current work. Table 4 indicates the modifications carried out in the present work along with the works reported in the literature. The enhancement of the Nu ratio in the proposed model is compared with the literature works, and their comparison is visually illustrated in Figure 23. In the normal turbulence condition, the value of Reynolds number is greater than 2500. In the present numerical study, the internal airflow is assumed to be turbulent; therefore, the higher Reynolds number is assumed, and the entire process simulation is carried out.

Table 4. Similar works in the literature.

Author	Modifications
Momin et al. [33]	Continuous V-shape rib
Saini et al. [34]	Continuous arc shape
Hans et al. [35]	Multi V shape
Aharwal et al. [36]	Inclined ribs with gap
Singh et al. [37]	V ribs with gap
Hans et al. [38]	Arc-shape with gap
Kumar et al. [39]	Multi-V ribs with gap
Pandey et al. [40]	Multi arc rib with gap
Bhattacharyya et al. [41]	Inclined turbulators
Chamoli et al. [42]	V-down shaped perforated baffles
Present work	Pin fin
Present work	Turbulators
Present work	Pin fin and Turbulators (PFT)

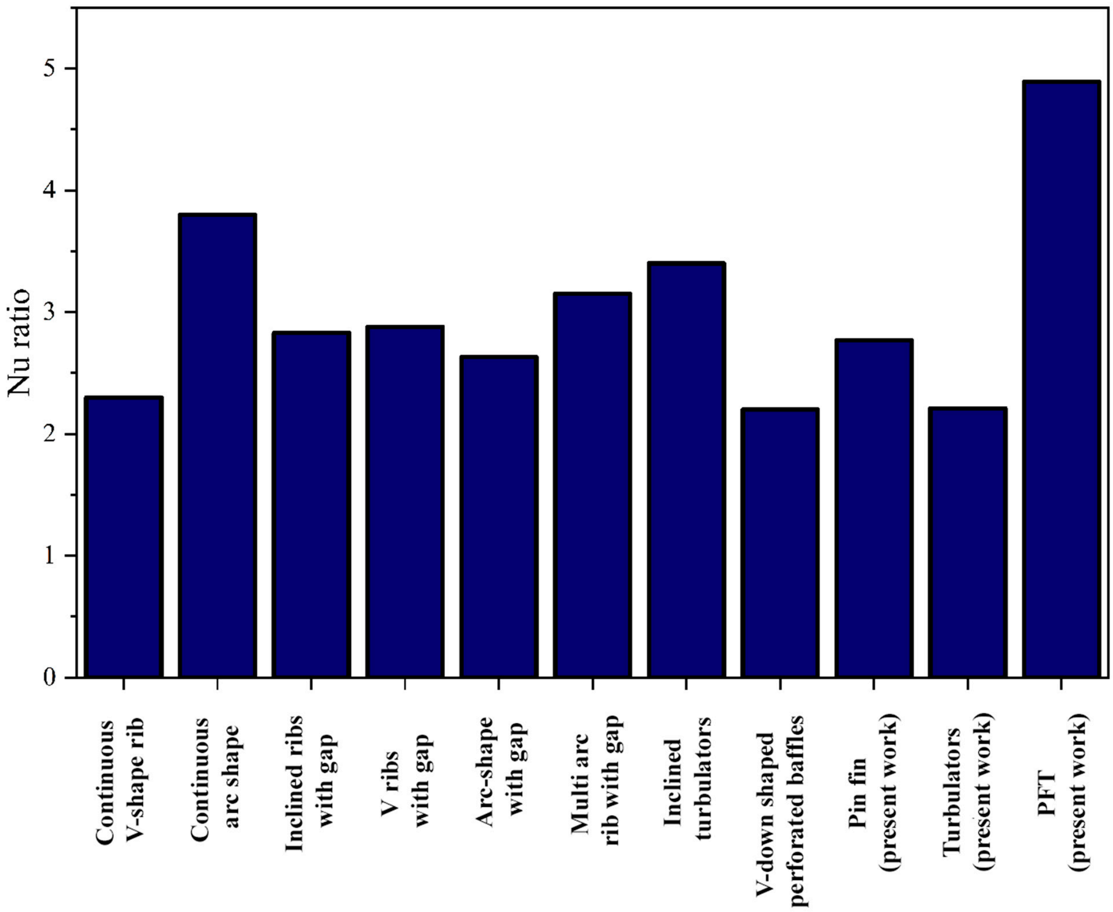

Figure 23. Effect of Fins and Turbulators on solar collector's Nu.

Generally, the solar collector's performance is measured based on thermal efficiency irrespective of different conditions and parameters. It is a crucial metric of the solar collector, directly impacting their ability to convert sunlight into heat energy effectively. The higher the efficiency, the more heat can be generated for a given amount of sunlight, resulting in a greater energy output. In line with this, the present study also follows the same approach and validates the effectiveness of the proposed solar collector based on its thermal efficiency.

Table 5 presents the comparative analysis of the proposed work with the previous results reported in the literature in terms of thermal efficiency, and the same is illustrated in Figure 24.

Table 5. Comparative analysis of current work with other similar works.

Author	Modifications	Reynold's Number (Re)	Mass Flux (kg/m^2 s)	Thermal Efficiency (%)
Sahu et al. [43]	Transverse Ribs (TR)	3000–12,000	-	83.5
Ramani et al. [44]	Porous Material (PM)	612–10,300	1.233–6.122	78.2
Lin et al. [45]	Wavelike absorbing plate parallel to the flow direction (WLF)	4600–5200	0.001–0.25	55.92
Lin et al. [45]	Wavelike absorbing plate perpendicular to the flow direction (WPF)	4600–5200	0.001–0.25	57.04
Lin et al. [45]	Cross-corrugated absorbing plates (CCP)	4600–5200	0.001–0.25	40.21
Present work	Pin fin	3000–15,000	2.75–13.845	81.79
Present work	Turbulators	3000–15,000	2.75–13.845	86.65
Present work	Pin fin and Turbulators (PFT)	3000–15,000	2.75–13.845	89.54

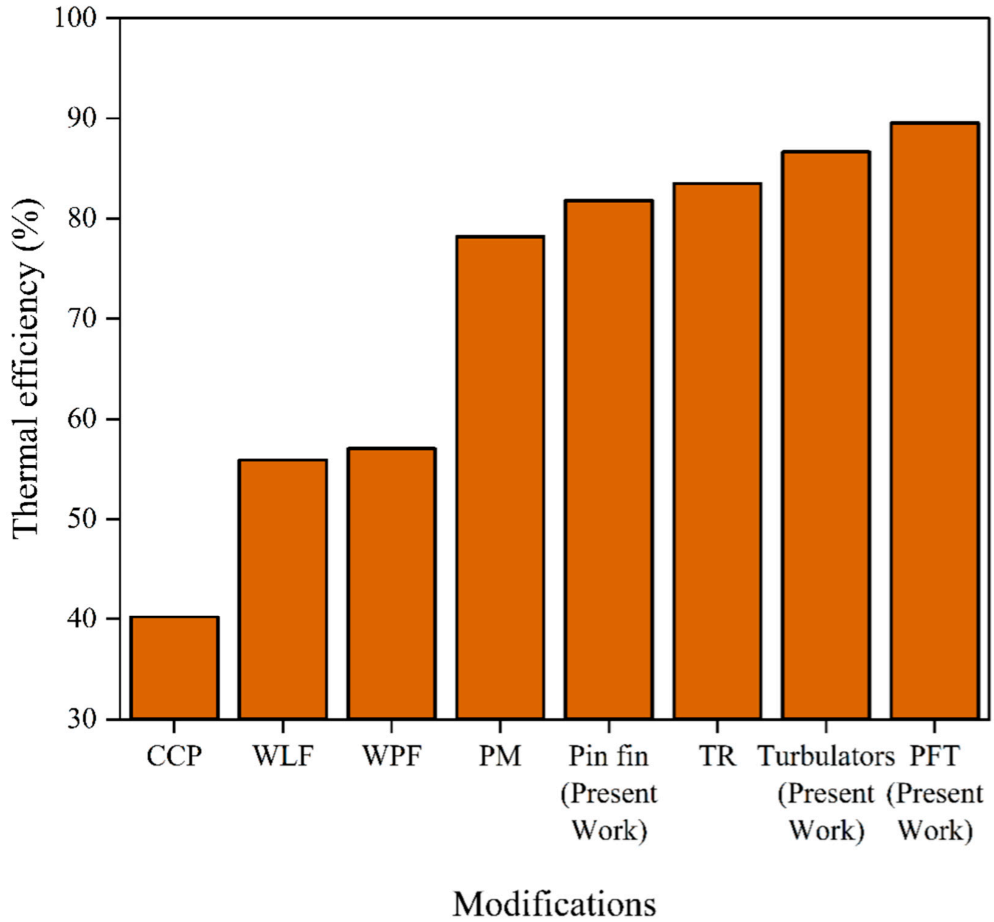

Figure 24. Comparison of thermal efficiency of the proposed work with similar studies.

Due to the higher thermal conductivity of CNT, the thermal energy transferred from the base plate to the circulating air is enhanced compared to conventional materials, resulting in a Nu ratio greater than unity. Combining pin fins and turbulators further increases this ratio significantly. The combination of pin fins and turbulators breaks the laminar sub layer and reduces the hydraulic diameter, resulting in a considerable improvement of the Nu and overall heat transfer. Additionally, the wavy and corrugated modifications of the proposed collectors significantly increase their thermal efficiency, as shown in Figure 24. Thus, CNT pin fins and turbulators have a high Nusselt ratio and augment the overall thermal efficiency of solar air collectors.

5. Conclusions

In the present work, a numerical investigation of solar thermal collector with pin fins and turbulators is presented. The proposed model enhances the heat transfer and improves efficiency. The numerical analysis carried out in the present work assumes that the bottom of the absorbing plate of the solar collector is perfectly insulated and has a minimum amount of heat losses. The study revealed that the Nusselt number is higher in all cases due to an augment in turbulent kinetic energy and its dissipation rate at higher Reynolds numbers. This increase in the Nusselt number also resulted in an enhanced useful heat energy transfer rate from the base plate.

The addition of pin fins decreased the hydraulic diameter of the collector, leading to increased Nusselt numbers for both the absorber plate and airflow. The utilization of fins resulted in considerable improvements in Nusselt numbers across all Reynolds numbers. The Nusselt number of a base plate with CNT pin fins and turbulators (with optimized parameters) was compared to that of a smooth plate, resulting in a 176% increase in Nusselt number with fins and a 122% increase with turbulators at certain values of Reynolds numbers.

The study also found that the proposed CNT pin fins and turbulators had a thermal efficiency of around 89.54% at the maximum mass flow rate of 0.96915 kg/s (3.49 m^3/h) and thermal efficiency of around 49.55% at the minimum mass flow rate of about 0.19383 kg/s (0.7 m^3/h). This obtained thermal efficiency value is higher than previous works reported in the literature. At a Reynolds number of 15,000, the higher value of Nusselt number attained with CNT pin fins and turbulators was 137.37, which is 211% higher than that of a conventional solar collector.

Author Contributions: Conceptualization, E.F.I.R., S.-C.K. and M.A.; methodology, E.F.I.R. and M.A.; software, E.F.I.R. and M.A.; validation, E.F.I.R., M.A., V.R., A.M.G. and S.R.S.; formal analysis, V.R.; data curation, E.F.I.R., S.-C.K. and M.A.; writing—original draft preparation, E.F.I.R. and M.A.; writing—review and editing, V.R. and S.-C.K.; supervision, A.M.G., S.-C.K. and S.R.S.; funding acquisition, S.R.S. and S.-C.K. All authors have read and agreed to the published version of the manuscript.

Funding: Woosong University's Academic Research Funding—2023.

Data Availability Statement: Not applicable.

Conflicts of Interest: The authors declare no conflict of interest.

Nomenclature

η_t	Thermal efficiency
Q_u	Energy gain
I_T	Incident solar thermal rays
A_p	Base plate surface area
ΔP	Pumping power
$\dot{m}$	Mass flow rate
Re	Reynold's Number
ρ	Density
T	Temperature
K_{eff}	Thermal conductivity
K	Turbulence kinetic energy
μ	Dynamic viscosity
e_t	Specific energy
h	Specific enthalpy
S_h	Hourly solar radiation
Nu	Nusselt number
P_r	Prandtl number
D_h	Hydraulic diameter
L	Base plate length

References

1. IEA. *Renewables 2022*; IEA: Paris, France, 2022.
2. Jradi, M.; Riffat, S. Medium Temperature Concentrators for Solar Thermal Applications. *Int. J. Low-Carbon Technol.* **2014**, *9*, 214–224. [CrossRef]
3. Zhang, D.; Li, J.; Gao, Z.; Wang, L.; Nan, J. Thermal Performance Investigation of Modified Flat Plate Solar Collector with Dual-Function. *Appl. Therm. Eng.* **2016**, *108*, 1126–1135. [CrossRef]
4. Tasmin, N.; Farjana, S.H.; Hossain, M.R.; Golder, S.; Mahmud, M.A.P. Integration of Solar Process Heat in Industries: A Review. *Clean Technol.* **2022**, *4*, 97–131. [CrossRef]
5. Sreekumar, A. Techno-Economic Analysis of a Roof-Integrated Solar Air Heating System for Drying Fruit and Vegetables. *Energy Convers. Manag.* **2010**, *51*, 2230–2238. [CrossRef]
6. Sánchez, M.M.; Lucas, M.; MartÍnez, P.; Sánchez, A.; Viedma, A. Climatic Solar Roof: An Ecological Alternative to Heat Dissipation in Buildings. *Sol. Energy* **2002**, *73*, 419–432. [CrossRef]
7. Amer, B.M.A.; Hossain, M.A.; Gottschalk, K. Design and Performance Evaluation of a New Hybrid Solar Dryer for Banana. *Energy Convers. Manag.* **2010**, *51*, 813–820. [CrossRef]

8. Saxena, A.; Agarwal, N.; Srivastava, G. Design and Performance of a Solar Air Heater with Long Term Heat Storage. *Int. J. Heat Mass Transf.* **2013**, *60*, 8–16. [CrossRef]
9. Liu, F.; Wang, J.; Liu, Y.; Wang, F.; Chen, Y.; Du, Q.; Sun, F.; Yang, N. Natural Convection Characteristics of Honeycomb Fin with Different Hole Cells for Battery Phase-Change Material Cooling Systems. *J. Energy Storage* **2022**, *51*, 104578. [CrossRef]
10. Xue, Y.; Ge, Z.; Du, X.; Yang, L. On the Heat Transfer Enhancement of Plate Fin Heat Exchanger. *Energies* **2018**, *11*, 1398. [CrossRef]
11. Singh, H.; Alam, T.; Haque Siddiqui, M.I.; Ashraf Ali, M.; Sagar, D. Experimental Investigation of Heat Transfer Augmentation Due to Obstacles Mounted in Solar Air Heater Duct. *Exp. Heat Transf.* **2022**, *35*, 1–20. [CrossRef]
12. Eismann, R.; Hummel, S.; Giovannetti, F. A Thermal-Hydraulic Model for the Stagnation of Solar Thermal Systems with Flat-Plate Collector Arrays. *Energies* **2021**, *14*, 733. [CrossRef]
13. Dhaundiyal, A.; Gebremicheal, G.H. The Stack Effect on the Thermal-Fluid Behaviour of a Solar Collector. *Energies* **2022**, *15*, 1188. [CrossRef]
14. Prasad, B.N.; Kumar, A.; Singh, K.D.P. Optimization of Thermo Hydraulic Performance in Three Sides Artificially Roughened Solar Air Heaters. *Sol. Energy* **2015**, *111*, 313–319. [CrossRef]
15. Kumar, B.V.; Manikandan, G.; Kanna, P.R.; Taler, D.; Taler, J.; Nowak-Ocłoń, M.; Mzyk, K.; Toh, H.T. A Performance Evaluation of a Solar Air Heater Using Different Shaped Ribs Mounted on the Absorber Plate—A Review. *Energies* **2018**, *11*, 3104. [CrossRef]
16. Singh, V.P.; Jain, S.; Karn, A.; Kumar, A.; Dwivedi, G.; Meena, C.S.; Dutt, N.; Ghosh, A. Recent Developments and Advancements in Solar Air Heaters: A Detailed Review. *Sustainability* **2022**, *14*, 12149. [CrossRef]
17. Alam, T.; Kim, M.-H. A Critical Review on Artificial Roughness Provided in Rectangular Solar Air Heater Duct. *Renew. Sustain. Energy Rev.* **2017**, *69*, 387–400. [CrossRef]
18. Qi, R.; Chen, F.; Xu, L.; Yu, J.; Chen, X. Effects of Reynolds Number on the Overall Characteristics of Flow and Heat Transfer in the Long Micro-Tube with Dimples. *Processes* **2022**, *10*, 2696. [CrossRef]
19. Li, H.; Kottke, V. Analysis of Local Shellside Heat and Mass Transfer in the Shell-and-Tube Heat Exchanger with Disc-and-Doughnut Baffles. *Int. J. Heat Mass Transf.* **1999**, *42*, 3509–3521. [CrossRef]
20. Habib, M.A.; Mobarak, A.M.; Attya, A.M.; Aly, A.Z. An Experimental Investigation of Heat-Transfer and Flow in Channels with Streamwise-Periodic Flow. *Energy* **1992**, *17*, 1049–1058. [CrossRef]
21. Skullong, S.; Thianpong, C.; Jayranaiwachira, N.; Promvonge, P. Experimental and Numerical Heat Transfer Investigation in Turbulent Square-Duct Flow through Oblique Horseshoe Baffles. *Chem. Eng. Process. Process Intensif.* **2016**, *99*, 58–71. [CrossRef]
22. Liou, T.-M.; Hwang, J.-J. Turbulent Heat Transfer Augmentation and Friction in Periodic Fully Developed Channel Flows. *J. Heat Transfer* **1992**, *114*, 56–64. [CrossRef]
23. Chang, W.; Wang, Y.; Li, M.; Luo, X.; Ruan, Y.; Hong, Y.; Zhang, S. The Theoretical and Experimental Research on Thermal Performance of Solar Air Collector with Finned Absorber. *Energy Procedia* **2015**, *70*, 13–22. [CrossRef]
24. Hu, J.; Liu, K.; Guo, M.; Zhang, G.; Chu, Z.; Wang, M. Performance Improvement of Baffle-Type Solar Air Collector Based on First Chamber Narrowing. *Renew. Energy* **2019**, *135*, 701–710. [CrossRef]
25. Chaichan, M.T.; Abaas, K.I.; Kazem, H.A. Design and Assessment of Solar Concentrator Distillating System Using Phase Change Materials (PCM) Suitable for Desertic Weathers. *Desalin. Water Treat.* **2016**, *57*, 14897–14907. [CrossRef]
26. Kumar Nougriaya, S.; Chopra, M.K.; Gupta, B.; Baredar, P. Stepped Solar Still: A Review on Designs Analysis. *Mater. Today Proc.* **2021**, *46*, 5647–5660. [CrossRef]
27. Yadav, A.S.; Bhagoria, J.L. A Numerical Investigation of Square Sectioned Transverse Rib Roughened Solar Air Heater. *Int. J. Therm. Sci.* **2014**, *79*, 111–131. [CrossRef]
28. Promthaisong, P.; Eiamsa-ard, S. Fully Developed Periodic and Thermal Performance Evaluation of a Solar Air Heater Channel with Wavy-Triangular Ribs Placed on an Absorber Plate. *Int. J. Therm. Sci.* **2019**, *140*, 413–428. [CrossRef]
29. Nagaraj, M.; Reddy, M.K.; Honnesara Sheshadri, A.K.; Karanth, K.V. Numerical Analysis of an Aerofoil Fin Integrated Double Pass Solar Air Heater for Thermal Performance Enhancement. *Sustainability* **2023**, *15*, 591. [CrossRef]
30. Renteria, J.D.; Nika, D.L.; Balandin, A.A. Graphene Thermal Properties: Applications in Thermal Management and Energy Storage. *Appl. Sci.* **2014**, *4*, 525–547. [CrossRef]
31. Abdelkader, T.K.; Zhang, Y.; Gaballah, E.S.; Wang, S.; Wan, Q.; Fan, Q. Energy and Exergy Analysis of a Flat-Plate Solar Air Heater Coated with Carbon Nanotubes and Cupric Oxide Nanoparticles Embedded in Black Paint. *J. Clean. Prod.* **2020**, *250*, 119501. [CrossRef]
32. Esmaeili, Z.; Akbarzadeh, S.; Rashidi, S.; Valipour, M.S. Effects of Hybrid Nanofluids and Turbulator on Efficiency Improvement of Parabolic Trough Solar Collectors. *Eng. Anal. Bound. Elem.* **2023**, *148*, 114–125. [CrossRef]
33. Ebrahim Momin, A.-M.; Saini, J.S.; Solanki, S.C. Heat Transfer and Friction in Solar Air Heater Duct with V-Shaped Rib Roughness on Absorber Plate. *Int. J. Heat Mass Transf.* **2002**, *45*, 3383–3396. [CrossRef]
34. Saini, S.K.; Saini, R.P. Development of Correlations for Nusselt Number and Friction Factor for Solar Air Heater with Roughened Duct Having Arc-Shaped Wire as Artificial Roughness. *Sol. Energy* **2008**, *82*, 1118–1130. [CrossRef]
35. Hans, V.S.; Saini, R.P.; Saini, J.S. Heat Transfer and Friction Factor Correlations for a Solar Air Heater Duct Roughened Artificially with Multiple V-Ribs. *Sol. Energy* **2010**, *84*, 898–911. [CrossRef]
36. Aharwal, K.R.; Gandhi, B.K.; Saini, J.S. Heat Transfer and Friction Characteristics of Solar Air Heater Ducts Having Integral Inclined Discrete Ribs on Absorber Plate. *Int. J. Heat Mass Transf.* **2009**, *52*, 5970–5977. [CrossRef]

37. Singh, S.; Chander, S.; Saini, J.S. Heat Transfer and Friction Factor Correlations of Solar Air Heater Ducts Artificially Roughened with Discrete V-down Ribs. *Energy* **2011**, *36*, 5053–5064. [CrossRef]
38. Hans, V.S.; Gill, R.S.; Singh, S. Heat Transfer and Friction Factor Correlations for a Solar Air Heater Duct Roughened Artificially with Broken Arc Ribs. *Exp. Therm. Fluid Sci.* **2017**, *80*, 77–89. [CrossRef]
39. Jaurker, A.R.; Saini, J.S.; Gandhi, B.K. Heat Transfer and Friction Characteristics of Rectangular Solar Air Heater Duct Using Rib-Grooved Artificial Roughness. *Sol. Energy* **2006**, *80*, 895–907. [CrossRef]
40. Pandey, N.K.; Bajpai, V.K. Varun Experimental Investigation of Heat Transfer Augmentation Using Multiple Arcs with Gap on Absorber Plate of Solar Air Heater. *Sol. Energy* **2016**, *134*, 314–326. [CrossRef]
41. Bhattacharyya, S.; Chattopadhyay, H.; Guin, A.; Benim, A.C. Investigation of Inclined Turbulators for Heat Transfer Enhancement in a Solar Air Heater. *Heat Transf. Eng.* **2019**, *40*, 1451–1460. [CrossRef]
42. Chamoli, S.; Thakur, N.S. Heat Transfer Enhancement in Solar Air Heater with V-Shaped Perforated Baffles. *J. Renew. Sustain. Energy* **2013**, *5*, 23122. [CrossRef]
43. Sahu, M.M.; Bhagoria, J.L. Augmentation of Heat Transfer Coefficient by Using 90° Broken Transverse Ribs on Absorber Plate of Solar Air Heater. *Renew. Energy* **2005**, *30*, 2057–2073. [CrossRef]
44. Ramani, B.M.; Gupta, A.; Kumar, R. Performance of a Double Pass Solar Air Collector. *Sol. Energy* **2010**, *84*, 1929–1937. [CrossRef]
45. Lin, W.; Gao, W.; Liu, T. A Parametric Study on the Thermal Performance of Cross-Corrugated Solar Air Collectors. *Appl. Therm. Eng.* **2006**, *26*, 1043–1053. [CrossRef]